

LEARNED IMAGE CODING FOR MACHINES: A CONTENT-ADAPTIVE APPROACH

Nam Le^{*†}, Honglei Zhang[†], Francesco Cricri[†], Ramin Ghaznavi-Youvalari[†],
Hamed Rezazadegan Tavakoli[†], Esa Rahtu^{*}

[†]Nokia Technologies, ^{*}Tampere University
Tampere, Finland

ABSTRACT

Today, according to the Cisco Annual Internet Report (2018-2023), the fastest-growing category of Internet traffic is machine-to-machine communication. In particular, machine-to-machine communication of images and videos represents a new challenge and opens up new perspectives in the context of data compression. One possible solution approach consists of adapting current human-targeted image and video coding standards to the use case of machine consumption. Another approach consists of developing completely new compression paradigms and architectures for machine-to-machine communications. In this paper, we focus on image compression and present an inference-time content-adaptive finetuning scheme that optimizes the latent representation of an end-to-end learned image codec, aimed at improving the compression efficiency for machine-consumption. The conducted experiments targeting instance segmentation task network show that our online finetuning brings an average bitrate saving (BD-rate) of -3.66% with respect to our pretrained image codec. In particular, at low bitrate points, our proposed method results in a significant bitrate saving of -9.85%. Overall, our pretrained-and-then-finetuned system achieves -30.54% BD-rate over the state-of-the-art image/video codec Versatile Video Coding (VVC) on instance segmentation.

Index Terms— Image coding for machines, learned image compression, content-adaptation, finetuning, video coding for machines

1. INTRODUCTION

It is predicted that half of global connected devices and connections will be for machines-to-machine (M2M) communications by 2023 [1]. There has been a tremendous improvement of coding efficiency in the recent iterations of the human-oriented video coding standards such as Versatile Video Coding (VVC) [2]. The performance of such codecs, however, remains questionable in the use cases where non-human agents, hereinafter *machines*, are the first-class consumers. To understand this problem, the Moving Picture Experts Group (MPEG) has recently issued a new Ad-hoc group

called Video coding for machines (VCM) [3] in the effort to study and standardize these use cases.

In response to this emerging challenge, many studies have been actively conducted to explore alternative coding solutions for the new use cases. There exist mainly two categories of solutions: adapting the traditional image and video codecs for machine-consumption [4, 5], and employing end-to-end learned codecs that are optimized directly for *machines* by taking advantage of the neural network (NN) based solutions [6, 7]. Each approach has its own pros and cons. Traditional video codec-based solutions, built upon mature technologies and broadly adopted standards, are often compatible with existing systems [4, 5]. However, it is difficult to optimize the overall performance of a system that consists of a traditional video codec and neural networks that perform machine tasks [6]. On the other hand, NN-based codecs are easier to optimize, though they may suffer from data domain shift at inference time, when the test data distribution differs from the distribution of the data used for training the learnable parameters.

In this work, we address the problem of domain shift at inference time for end-to-end learned NN-based solutions. We propose a content-adaptive fine-tuning technique that can enhance the coding efficiency on-the-fly at the inference stage without modifying the architecture or the learned parameters of the codec. We demonstrate that the proposed method, as a complementary process, can improve the performance of a learned image codec targeting instance segmentation by saving up to -9.85% in bitrate.

2. RELATED WORK

End-to-end learned approaches aimed at improving the task performance on the outputs of the codec, have been studied in some recent works. Learned codecs that are optimized for both human and machine consumption are proposed in [8] and [7], either by integrating the semantic features into the bitstream [8] or by adapting the targeted task networks to the learned latent representation [7]. Concentrating solely on machine-consumption use cases, the codecs presented in [6] achieve state-of-the-art coding performance without any

modifications to the task networks. The above methods improve the task performance by designing new codecs trained on a certain amount of training data, which may have a different distribution than that of the test data at inference time. Our proposed method adapts only the transmitted data to the input content, hence alleviating the data domain shift while the codec remains unchanged.

Inference-time finetuning schemes have already been explored in numerous works in the context of image compression. The goal is to optimize some parts of the codec in order to maximize its performance on the given input test data. This operation is performed on the encoder side, and the subject of optimization may be the encoder itself, the output of the encoder, or the decoder. In [9, 10], the post-processing filter is finetuned at decoder side by using weight-updates signaled from the encoder to the decoder at inference time. Techniques of latent tensor overfitting for better human consumption are presented in [11, 12], aiming at reducing the distortion in the pixel domain. Such approaches are useful for enhancing the fidelity in the pixel domain and their application is straightforward, as the ground-truth at the encoder-side is readily available (the uncompressed image itself). However, similar techniques are not directly applicable to a NN-based codec that targets machine tasks, where neither the ground-truth nor the task networks are available at the encoder side. In this paper, we propose a content-adaptive finetuning technique that can further improve the performance of a NN-based codec for machine consumption.

3. PROPOSED METHOD

An image coding for machines (ICM) codec aims to achieve optimal task network performance given a targeted bitrate, as opposed to the traditional codecs which are optimized for the visual quality. In this work, we propose a content-adaptive finetuning scheme that further enhances the coding efficiency of NN-based ICM codecs. As a concrete example, we apply this technique on a baseline ICM codec described below.

3.1. Baseline ICM system

We use an ICM system based on [6] as a baseline. Such system consists of three main components: a probability model, a task network representing the “machine”, and an autoencoder. The overview of this system is presented in Fig. 1. To simplify the experiments, while still following the same principles proposed in [6], our system has some architectural adjustments which are described in the next paragraphs.

Probability model estimates the probability distribution and the bitrate of the data to be compressed. Instead of the probability model in [6], we incorporate a probability model based on the method proposed for a lossless image coding system [13], in which a N -level-downsampled version of the input image $z^{(1)}$ is encoded to achieve a higher compression

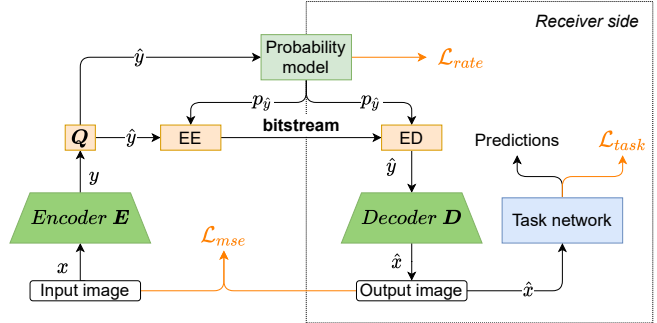


Fig. 1. System architecture of the baseline Image Coding for Machines system. “EE” and “ED” denote arithmetic entropy encoder and decoder, respectively.

rate. For each level of downsampling, the probability model learns the conditional distributions $p(z^{(l)}|z^{(l+1)})$, where $z^{(l+1)}$ denotes the downsampled image by a factor of 2 of $z^{(l)}$, and $l \in [1, N]$. The bitstream at each level is coded using the corresponding predicted conditional distribution with the lower resolution image as the context. These bitstreams can perfectly reconstruct $z^{(1)}$ from $z^{(N)}$. We apply this coding pipeline to losslessly compress the quantized latent \hat{y} in our base ICM system. The bitrate of the coded bitstream is estimated by the Shannon cross-entropy:

$$\mathcal{L}_{rate} = \mathbb{E}_{\hat{y} \sim m_{\hat{y}}} [-\log_2 p_{\hat{y}}(\hat{y})], \quad (1)$$

where $m_{\hat{y}}$ denotes the true distribution of input tensor \hat{y} and $p_{\hat{y}}(\hat{y})$ denotes the predicted distribution of \hat{y} .

Task network is based on Mask R-CNN [14] for instance segmentation. This network is pre-trained and kept unmodified in our experiments. It provides predictions for task performance evaluation and task loss \mathcal{L}_{task} during the training of the codec. The task loss is defined as the training loss of the Mask R-CNN network:

$$\mathcal{L}_{task} = \underbrace{\mathcal{L}_{cls} + \mathcal{L}_{reg}}_{\text{classifier branch}} + \underbrace{\mathcal{L}_{preg} + \mathcal{L}_{obj}}_{\text{RPN branch}} + \underbrace{\mathcal{L}_{mask}}_{\text{mask branch}}, \quad (2)$$

where \mathcal{L}_{cls} , \mathcal{L}_{reg} , \mathcal{L}_{preg} , \mathcal{L}_{obj} and \mathcal{L}_{mask} denote classification loss, regression loss, region proposal regression loss, objectness loss and mask prediction loss, respectively. These losses come from the 3 branches of the network architecture: classifier branch, region proposal network (RPN) branch, and mask predictor branch, respectively. Readers are referred to [14] for further information about these components.

Autoencoder performs the lossy encoding and decoding operations. Together with the probability model and the arithmetic codec, it forms the “codec” in the ICM system. It is a convolutional neural network (CNN) with residual connections as illustrated in Fig. 2. This is an almost identical network to the one described in [6], except for the number

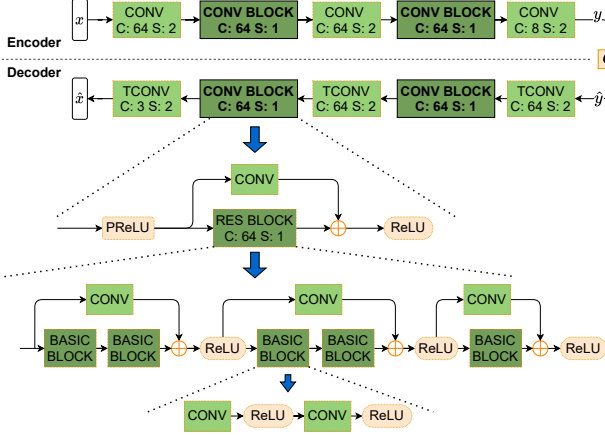


Fig. 2. Auto-encoder architecture. The convolutional blocks are illustrated by sharp rectangles. “TCONV” denotes the transposed convolutional layers. In each convolutional block, “S” denotes the stride and “C” denotes the number of output channels for all of the children blocks. These values are inherited from the parent block if not stated otherwise.

of channels in the last layer of the encoder. We use a 6-bit uniform quantizer in this work, denoted as $Q(\cdot)$. The learned encoder takes the uncompressed image x as input and transforms it into a more compressible latent representation $y = E(x; \theta_E)$, where θ_E denotes the learned parameters of the encoder. The quantized latent $\hat{y} = Q(y)$ is submitted to the probability model for a distribution estimation, which is used as the prior for the entropy coding. The decoder transforms the latent data back to the pixel domain as the reconstructed image $\hat{x} = D(\hat{y}; \theta_D)$.

Training strategy: the above “codec” is trained to optimize the multi-task loss function:

$$\mathcal{L}_{train} = w_{rate} \cdot \mathcal{L}_{rate} + w_{task} \cdot \mathcal{L}_{task} + w_{mse} \cdot \mathcal{L}_{mse}, \quad (3)$$

where \mathcal{L}_{rate} and \mathcal{L}_{task} are specified by Eq. (1) and Eq. (2), \mathcal{L}_{mse} denotes the mean square error between x and \hat{x} , and w_{rate} , w_{task} , w_{mse} are the scalar weights for the above losses, respectively. These values follow the same configuration proposed in [6], in order to delicately handle the loss terms balancing problem and at the same time train the codec to achieve good efficiency on a wide variety of targeted bitrates.

3.2. Online latent tensor finetuning

At the inference stage, it is possible to further optimize the system by adapting it to the content being encoded. This way, even better rate-task performance trade-offs can be achieved. However, this content-adaptive optimization should be done only for the components at the encoder-side, otherwise additional signals containing the updates need to be sent to the

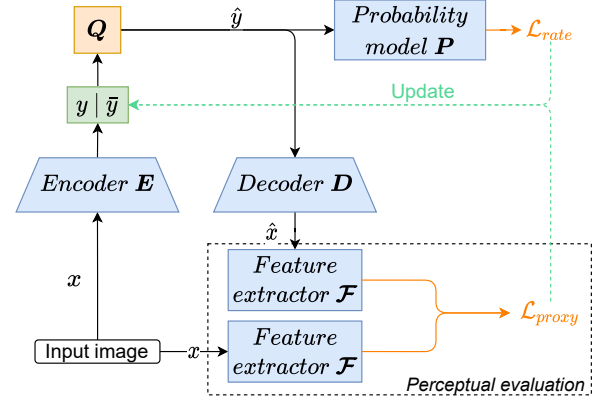


Fig. 3. Online latent tensor finetuning pipeline

decoder-side, resulting in bitrate overhead. Instead of finetuning the encoder, it is sufficient to finetune the latent tensor y , by back-propagating gradients of the loss with respect to elements of y through the frozen decoder and probability model. However, at the inference stage, \mathcal{L}_{task} is unknown to the encoder since the ground-truth for the tasks is not available. Furthermore, the task network is only available on the decoder side and not on the encoder side. We hypothesize that the intermediate layer features of the task networks should be correlated to those of other vision tasks to a certain degree. Therefore, we propose finetuning y by using the gradients of the following finetuning loss:

$$\tilde{\mathcal{L}}_{total} = \bar{w}_{rate} \cdot \tilde{\mathcal{L}}_{rate} + \bar{w}_{proxy} \cdot \tilde{\mathcal{L}}_{proxy}, \quad (4)$$

where \bar{w}_{rate} , \bar{w}_{proxy} denote the weights for the finetuning loss terms, $\tilde{\mathcal{L}}_{rate}$ is similar to \mathcal{L}_{rate} , and $\tilde{\mathcal{L}}_{proxy}$ denotes a feature-based perceptual loss which acts as a proxy for the task loss \mathcal{L}_{task} . Fig. 3 illustrates our finetuning scheme. In our experiments, we used a VGG-16 [15] model pretrained on ImageNet [16] as the feature extractor. The perceptual loss term $\tilde{\mathcal{L}}_{proxy}$ is given by

$$\tilde{\mathcal{L}}_{proxy} = \text{MSE}(\mathcal{F}_2(x), \mathcal{F}_2(\hat{x})) + \text{MSE}(\mathcal{F}_4(x), \mathcal{F}_4(\hat{x})), \quad (5)$$

where MSE denotes the mean square error calculation and $\mathcal{F}_i(t)$ denotes the input of the i^{th} Max Pooling layer of the feature extractor given the input t . The feature extraction is visualized in Fig. 4. The finetuning process is described by algorithm 1. By using the gradients from $\tilde{\mathcal{L}}_{total}$ w.r.t y , the system learns to update y for better coding efficiency without the knowledge of the task network or ground-truth annotations, which makes it a sensible solution.

4. EXPERIMENTS

4.1. Experimental setup

For the baseline system, we followed the same training setup as in [6]. We used Cityscapes dataset [17] which contains

Algorithm 1: Latent finetuning at inference stage

Input: Input image x , learning rate η , number of iterations n , loss weights $\bar{w}_{rate}, \bar{w}_{proxy}$

Output: Content-adapted latent tensor \bar{y}

```
function FeatureLoss ( $t_1, t_2$ ):
  return MSE( $\mathcal{F}_2(t_1), \mathcal{F}_2(t_2)$ ) +
         MSE( $\mathcal{F}_4(t_1), \mathcal{F}_4(t_2)$ )
```

```
 $\bar{y} = E(x)$ 
// Finetuning iterations
for  $i = 1 \rightarrow n$  do
   $\hat{y} = Q(\bar{y})$ 
   $p_{\hat{y}} = P(\hat{y})$ 
   $\hat{x} = D(\hat{y})$ 
   $\mathcal{L}_{rate} = \mathbb{E}_{\hat{y} \sim m_{\hat{y}}} [-\log_2 p_{\hat{y}}(\hat{y})]$ 
   $\mathcal{L}_{proxy} = \text{FeatureLoss}(x, \hat{x})$ 
   $\mathcal{L}_{total} = \bar{w}_{rate} \cdot \mathcal{L}_{rate} + \bar{w}_{proxy} \cdot \mathcal{L}_{proxy}$ 
   $\bar{y} = \bar{y} - \eta \cdot \nabla_{\bar{y}} \mathcal{L}_{total}$ 
end
return  $\bar{y}$ 
```

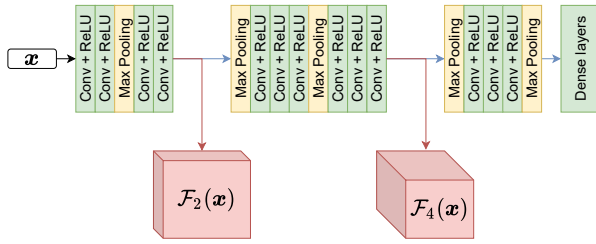


Fig. 4. Feature extraction using VGG-16 (Eq. (5)).

uncompressed images of resolution 2048×1024 , in two subsets: *train* and *val*. We trained the baseline system described in the previous section on the *train* set of 2975 images for these classes: *car, person, bicycle, bus, truck, train, motorcycle*. The instance segmentation task network is provided by Torchvision¹. The system is implemented with Pytorch 1.5.

After every training epoch, we evaluated the coding efficiency with respect to the task performance of the model on 500 images of *val* set. We use mean average precision (mAP@[0.5:0.05:0.95], described in [17]) and bits per pixel (BPP) as the metrics for task performance and bitrate, respectively. Note that because of the varying weights for the loss terms throughout the training, the codec is able to provide different trade-offs that cover a wide range of bitrates. A Pareto front set of these checkpoints (i.e., saved models of the epochs) was selected and visualized in Fig. 5 as “ICM baseline”. For simplicity, we report the bitrate estimations

¹The pre-trained models can be found at <https://pytorch.org/docs/stable/torchvision/models.html>

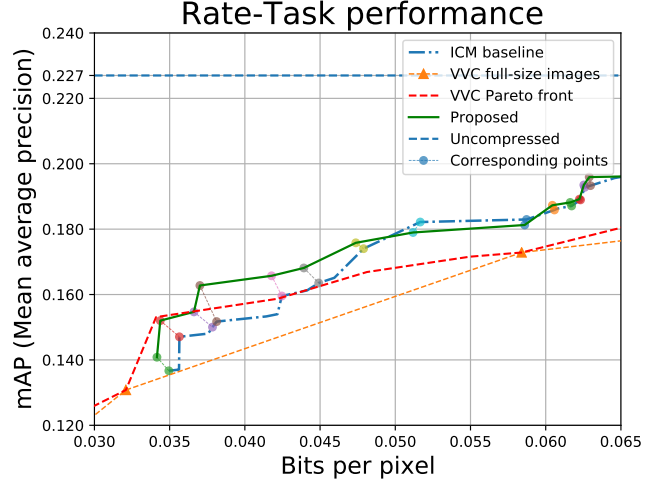


Fig. 5. Rate-performance curves on low bitrates. The small dashed lines connect the baseline checkpoints and their respective finetuned versions.

using the Shannon entropy in Eq. (1) instead of the bitrates arising from the actual bitstream lengths. In practice, we have verified that the differences between them are negligible.

We also provide evaluation results using the state-of-the-art video codec VVC (reference software VTM-8.2², All-intra configuration), under JVET common test conditions [18]. The *val* set is coded in 28 settings of 7 quantization parameters (22, 27, 32, 37, 42, 47 and 52) and 4 downsampling factors (1, 0.75, 0.50 and 0.25) to achieve different output bitrates. The 28 coded versions of the original input are then evaluated for task performance. The Pareto front from these 28 pairs of bitrate and corresponding task performance is clipped for the relevant bitrate range and visualized in Fig. 5 as “VVC Pareto front”. Additionally, “VVC full-size images” is illustrated representing only the data points that are coded without downsampling, i.e. common use case of VVC.

Since the baseline model already has a significant performance gain in the higher bitrates, we focus on finetuning the coding efficiency at low bitrates in this work. Thus, we used the learning rate $\eta = 10^{-4}$ to prevent large changes to latent entropy values, which correspond to the bitrates. We observed that the losses converge after a few iterations on many samples, therefore the number of iterations $n = 30$ and loss weights $\bar{w}_{rate} = 1$ and $\bar{w}_{proxy} = 0.1$ are empirically chosen in order to achieve a feasible runtime. More sophisticated algorithms and strategies can be applied to this process.

At the inference stage, for every baseline checkpoint, we finetune the latent y of images in the *val* set individually using the Adam optimizer [19]. Then the finetuned latent \bar{y} is

²https://vcgit.hhi.fraunhofer.de/jvetVVCSoftware_VTM

Table 1. BD-rates w.r.t task performance of our proposed method on different bitrates.

Compared to	Bitrate (BPP)			Total
	< 0.05	[0.05, 0.1]	> 0.1	
ICM baseline	-9.85%	-0.71%	-0.09%	-3.66%
VVC Pareto	-4.81%	-40.90%	-66.42%	-25.46%
VVC full-size	-11.64%	-44.82%	-70.51%	-30.54%

evaluated. The average coding efficiency of the finetuned latents is reported over the whole *val* set for each checkpoint. A Pareto front set from the finetuned data points is selected to compare with the baseline and is visualized in Fig. 5 as the performance of our method.

4.2. Experimental results

The finetuning at inference time offers a bitrate saving, indicated by Bjøntegaard Delta (BD)-rate [20], of up to -9.85%. The average bitrate saving over the whole evaluated bitrate range is -3.66%. In low bitrates (< 0.05 BPP), this process significantly boosts the coding efficiency as shown in Fig. 5.

A summary of the BD-rates in different bitrate ranges is presented in Table 1. Apart from the coding performance enhancement achieved by the proposed finetuning technique, this table also shows impressive BD-rates of up to -66.42% at low bitrates and -25.46% on average when compared to the VVC codec for machine-consumption. As a reference, this measurement of the segmentation codec in [6], which is a different codec than our ICM baseline, measured on the same bitrate range as in our evaluation³ is -23.92% on average. The finetuning of 30 iterations takes around 2 hours for each checkpoint on the whole *val* set, or \approx 14 seconds per image, with a NVIDIA RTX 2080Ti GPU.

In Fig. 6, the finetuning on the baseline outputs targeting low bitrates clearly show that there are structural modifications around the edge areas of the objects in the images, consequently resulting into higher coding performance. The outputs targeting high bitrates are only negligibly modified, which aligns with the reported insignificant bitrate saving in this range. Fig. 7 shows an example of the segmentation error being reduced after finetuning.

5. CONCLUSIONS

The proposed content-adaptive finetuning technique can significantly improve the coding performance especially for low targeted bitrates. This technique does not require a differentiable encoder and it is not dependent on the availability of the task network or task ground-truth, therefore it can be easily adopted into most computer vision workflows that employ

³Determined by the minimum and maximum achievable bitrates using our trained models: [0.034, 0.148]

NN-based coding. Additionally, the comparison to the traditional VVC codec confirms the superior coding performance of the machine-targeted codec for machine-consumption.

To further improve our technique, future work could explore different configurations to magnify the enhancement of coding efficiency in a wider range of bitrates. Furthermore, the effectiveness of this finetuning technique could be verified for more computer vision tasks, either separately or on the same finetuned output.

6. REFERENCES

- [1] “Cisco annual internet report (2018–2023) white paper,” Updated: Mar 2020.
- [2] B. Bross, J. Chen, S. Liu, and Y.-K. Wang, “Versatile Video Coding (draft 8),” *Joint Video Experts Team (JVET), Document JVET-Q2001*, Jan 2020.
- [3] Y. Zhang, M. Rafie, and S. Liu, “Use cases and requirements for video coding for machines,” *ISO/IEC JTC 1/SC 29/WG 2*, Oct 2020.
- [4] B. Brummer and C. de Vleeschouwer, “Adapting JPEG XS gains and priorities to tasks and contents,” in *2020 IEEE/CVF Conference on Computer Vision and Pattern Recognition Workshops (CVPRW)*, 2020, pp. 629–633.
- [5] K. Fischer, F. Brand, C. Herglotz, and A. Kaup, “Video coding for machines with feature-based rate-distortion optimization,” *IEEE 22nd International Workshop on Multimedia Signal Processing*, p. 6, September 2020.
- [6] N. Le, H. Zhang, F. Cricri, R. Ghaznavi-Youvalari, and E. Rahtu, “Image coding for machines: An end-to-end learned approach,” *2021 IEEE International Conference on Acoustics, Speech and Signal Processing (ICASSP)*, 2021, (in press).
- [7] N. Patwa, N. Ahuja, S. Somayazulu, O. Tickoo, S. Varadarajan, and S. Koolagudi, “Semantic-preserving image compression,” in *2020 IEEE International Conference on Image Processing (ICIP)*, pp. 1281–1285.
- [8] S. Luo, Y. Yang, Y. Yin, C. Shen, Y. Zhao, and M. Song, “DeepSIC: Deep semantic image compression,” in *Neural Information Processing*, L. Cheng, A. C. S. Leung, and S. Ozawa, Eds. 2018, Lecture Notes in Computer Science, pp. 96–106, Springer International Publishing.
- [9] Y.-H. Lam, A. Zare, F. Cricri, J. Lainema, and M. M. Hannuksela, “Efficient adaptation of neural network filter for video compression,” in *Proceedings of the 28th ACM International Conference on Multimedia*. 2020, MM ’20, pp. 358–366, Association for Computing Machinery.
- [10] Y. Hong Lam, A. Zare, C. Aytakin, F. Cricri, J. Lainema, E. Aksu, and M. Hannuksela, “Compressing weight-updates for image artifacts removal neural networks,” in *IEEE/CVF Conference on Computer Vision and Pattern Recognition Workshops*, 2019.

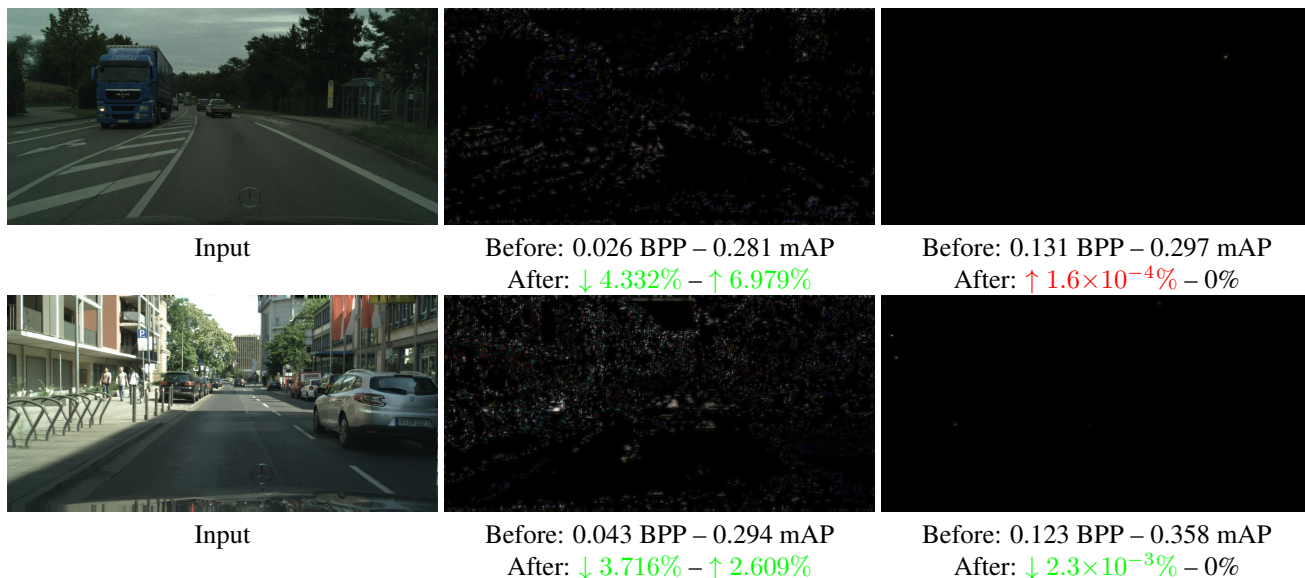


Fig. 6. Finetuning effects on different targeted bitrates. In each row, the leftmost image is the uncompressed input and the other images are the ℓ_1 -norm difference images between the baseline outputs and the finetuned ones for different targeted bitrates. The gains after finetuning are given under the images. The finetuning process modifies the areas around the edges and surfaces of the objects in low-bitrate targeted output, which allows for higher coding gains.

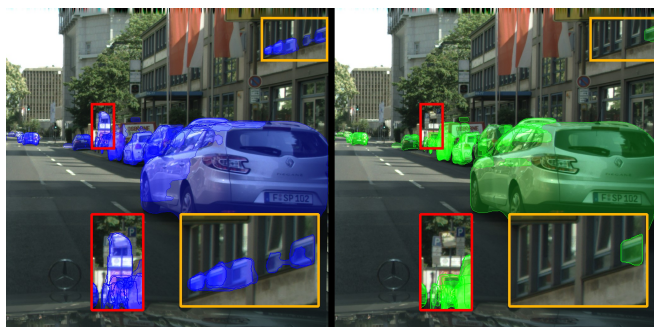


Fig. 7. Error reduction of segmentation before and after the finetuning. Left: baseline results, right: finetuned results.

- [11] N. Zou, H. Zhang, F. Cricri, H. R. Tavakoli, J. Lainema, M. Hannuksela, E. Aksu, and E. Rahtu, “ L^2C – learning to learn to compress,” *IEEE 22nd International Workshop on Multimedia Signal Processing*, 2020.
- [12] J. Campos, S. Meierhans, A. Djelouah, and C. Schroers, “Content adaptive optimization for neural image compression,” in *IEEE/CVF Conference on Computer Vision and Pattern Recognition Workshops*, 2019.
- [13] H. Zhang, F. Cricri, H. R. Tavakoli, N. Zou, E. Aksu, and M. M. Hannuksela, “Lossless image compression using a multi-scale progressive statistical model,” in *Proceedings of the Asian Conference on Computer Vision (ACCV)*, November 2020.
- [14] K. He, G. Gkioxari, P. Dollár, and R. Girshick, “Mask R-CNN,” in *2017 IEEE International Conference on Computer Vision (ICCV)*, 2017, pp. 2980–2988.
- [15] S. Liu and W. Deng, “Very deep convolutional neural network based image classification using small training sample size,” in *2015 3rd IAPR Asian Conference on Pattern Recognition (ACPR)*, 2015, pp. 730–734.
- [16] O. Russakovsky, J. Deng, H. Su, J. Krause, S. Satheesh, S. Ma, Z. Huang, A. Karpathy, A. Khosla, M. Bernstein, A. C. Berg, and L. Fei-Fei, “ImageNet large scale visual recognition challenge,” *International Journal of Computer Vision (IJCV)*, vol. 115, no. 3, pp. 211–252, 2015.
- [17] M. Cordts, M. Omran, S. Ramos, T. Rehfeld, M. Enzweiler, R. Benenson, U. Franke, S. Roth, and B. Schiele, “The cityscapes dataset for semantic urban scene understanding,” in *2016 IEEE Conference on Computer Vision and Pattern Recognition (CVPR)*. 2016, pp. 3213–3223, IEEE.
- [18] F. Brossen, J. Boyce, K. Suehring, X. Li, and V. Seregin, “JVET common test conditions and software reference configurations for sdr video,” *Joint Video Experts Team (JVET)*, Document: JVET-N1010, March 2019.
- [19] D. P. Kingma and J. Ba, “Adam: A method for stochastic optimization,” in *International Conference on Learning Representations (ICLR) 2015*.
- [20] G. Bjontegaard, “Calculation of average psnr differences between RD-curves,” *ITU-T Video Coding Experts Group (VCEG)*, 2001.